NEW TECHNIQUE FOR PROCESSING DATA OBTAINED WITH A M–124 OZONOMETER

M.N. Eremenko, M.Yu. Kataev, and A.A. Mitsel'

Institute of Atmospheric Optics,
Siberian Branch of the Russian Academy of Sciences, Tomsk
Received July 17, 1998

A new technique is presented for processing data obtained from broad-band measurements of direct sunlight in order to increase the bulk of experimental information. The technique is based on the method of moments. It allows reconstruction of the total content of the gaseous constituent, the effective height of a layer, and its halfwidth. In order to reveal peculiarities and potentialities of the new technique as applied to reconstruction of the parameters sought, numerical simulations have been performed. Besides, the technique has been applied to process real data obtained with a M–124 ozonometer.

INTRODUCTION

M–124 device is widely used at Russian ozonometric stations to measure the total ozone content (TOC).[1,2] This device is a broad-band photometer with three spectral channels at 300 (21), 326 (21), and 348 (30) nm (widths of the corresponding filter passbands are given in parentheses). The technique of TOC measurements relies on the use of nomograms of signals from the first and second channels as functions of the sun zenith angle and n_3 content in the atmosphere. The nomogram covers the TOC range from 0.2 to 0.6 atm·cm. The third channel is used for calibration and measurement of the solar flux. The method of nomograms has shown its efficiency for the "unperturbed" atmosphere. However, natural "disasters," such as volcanic eruptions, distort the results of TOC estimation (such distortions cannot be envisioned and allowed for in nomograms). This means that uncontrollable errors can arise in TOC measurements.

The new technique for processing signals from a M–124 ozonometer is presented in this paper. It enables one 1) to eliminate the above-indicated drawback; 2) to estimate the depth of the aerosol and molecular atmosphere in addition to TOC measurements; 3) to perform fast analysis of the ozone profile.

Note that similar technique (the method of moments) has been already applied to quasimonochromatic measurements of direct sunlight.[2] However, this method has not been studied in detail in Ref. 2; and numerical simulation for revealing its peculiarities and potentialities has not been performed yet. "esides, the aerosol and molecular depths were supposed predetermined in Ref. 2.

The application of this new technique to processing signals from l –124 compiled during the passed period of measurements will allow us to reveal statistical regularities in TOC behavior, heights of the maximum in the ozone profile and its width with varying aerosol optical depth.

ESTIMATION OF THE OPTICAL DEPTH

The direct solar radiation fixed by a M–124 device is related to the atmospheric parameters as follows:

$$I(\lambda_j, \varphi) = c(\lambda_j) \int\limits_{\Delta\lambda} I_0(\lambda')\, T_f(\lambda' - \lambda_j) \times$$

$$\times\, T_{ma}(\lambda', \varphi)\, T_g(\lambda', \varphi)\, T_{oz}(\lambda', \varphi)\, d\lambda', \qquad (1)$$

where φ is the zenith angle of the Sun; $I_0(\lambda')$ is the intensity of the extraterrestrial sunlight; $T_f(\lambda' - \lambda)$ is the filter transmission; λ_j is the wavelength of the jth channel; $T_{ma}(\lambda' - \lambda)$ is the transmission of the molecular plus aerosol atmosphere; $T_{oz}(\lambda' - \lambda)$ is the ozone transmission; $T_g(\lambda' - \lambda)$ is the transmission of "interfering" gases (except n_3), which contribute into extinction of radiation; $c(\lambda_j)$ is the instrumental constant at the wavelength λ_j (j = 1, 2, 3).

Here we suppose that

$$\int T_f(\lambda' - \lambda_j)\, d\lambda' = 1.$$

The transmission of the ith attenuating atmospheric constituent can be presented as

$$T_i(\lambda, \varphi) = \exp\{-\tau_i(\lambda, \varphi)\}, \qquad (2)$$

where

$$\tau_i(\lambda, \varphi) = \int\limits_0^{H_{atm}} B(h, \varphi)\, \alpha_i(\lambda, h)\, dh; \quad i = a, m, g, oz. \qquad (3)$$

Here $B(h, \varphi)$ is the function of a path having the form

$$B(h, \varphi) = \frac{(h + R)\, n(h)}{\sqrt{(h + R)^2\, n^2(h) - R^2\, n_0^2 \sin^2 \varphi}}, \qquad (4)$$

where $\alpha_i(\lambda, h)$ is the volume extinction coefficient; R is the Earth's radius; $n(h)$ is the refractive index; H_{atm} is the top height of the atmosphere.

0235-6880/99/01 76-05 $02.00

Figure 1 demonstrates the calculated wavelength dependence of the optical depth of vertical column for the gas under study $\tau_{oz}(\lambda)$, the aerosol atmosphere $\tau_a(\lambda)$, "interfering" gases $\tau_g(\lambda)$, and the molecular atmosphere $\tau_m(\lambda)$. The transmission functions of optical filters are also given here. The initial data taken for calculations are the following: the ozone absorption coefficient $K_{oz}(\lambda)$ borrowed from Ref. 3; the ozone profile $\rho(h)$ borrowed from Refs. 4 and 5 ($W = 300$ D.u.); $\alpha_a(\lambda)$ corresponding to the model of the background aerosol[6]; the air density for $\tau_m(\lambda)$ calculation corresponding to the midlatitude summer model.[7] Two conclusions can be drawn from analysis of data shown in Fig. 1: (1) the optical depth $\tau_g(\lambda)$ of the "interfering" gases is small as compared with $\tau_{oz}(\lambda)$, $\tau_a(\lambda)$, and $\tau_m(\lambda)$. Therefore, the contribution of the "interfering" gases into the total intensity can be neglected and eliminated from further consideration; (2) the optical depths $\tau_a(\lambda)$ and $\tau_m(\lambda)$ can be considered wavelength–independent (or weakly dependent) within the filter passbands $T_{f1}(\lambda)$, $T_{f2}(\lambda)$, and $T_{f3}(\lambda)$.

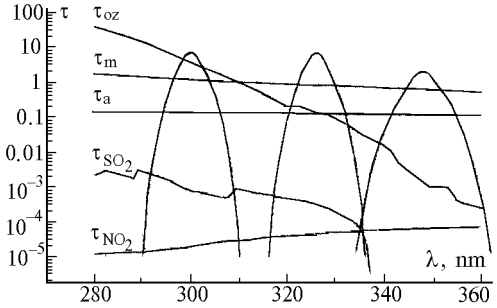

FIG. 1. The norHalized wavelength dependence of the optical depth of vertical coluHn of the gas under study $\tau_{oz}(\lambda)$, the aerosol atHosphere $\tau_a(\lambda)$, interfering gases $\tau_g(\lambda)$, and the Holecular atHosphere $\tau_m(\lambda)$, along with the transHission functions of the optical filters.

With regard for the above-said, Eq. (1) can be presented as

$$I(\lambda_j, \varphi) = c(\lambda_j)\, T_{ma}(\lambda_j, \varphi) \times \times \int_{\Delta\lambda} I_0(\lambda')\, T_f(\lambda' - \lambda_j)\, T_{oz}(\lambda')\, d\lambda'. \quad (5)$$

"elow we suppose the calibration constants $c(\lambda_j)$ being the same for all the channels (see Refs. 1, 2, and 8) and equal to C. "esides, the constant C is supposed to be known.

The integral in Eq. (5) is approximated by the following expression:

$$\int_{\Delta\lambda} I_0(\lambda')\, T_f(\lambda' - \lambda_j)\, T_{oz}(\lambda')\, d\lambda' = = \exp\{(-\beta_j\, (W(\varphi))^{n_j}\}. \quad (6)$$

Here β_j has the meaning of the effective ozone absorption coefficient per unit TOC; n_j is the parameter; $W(\varphi)$ is the total ozone content along the path in the atmospheric layer between the sun and the instrument:

$$W(\varphi) = \int_0^{H_{atm}} \frac{(h + R)\, \rho(h)\, dh}{\sqrt{(h + R)^2 - R^2 \sin^2 \varphi}}; \quad (7)$$

$\rho(h)$ is the ozone concentration profile.

In Eq. (7), we have neglected the refractive index $n(h)$ (see Eq. (4)).

The parameters β_j and n_j of the model (6) are calculated on the basis of data on the filter transmission $T_{fj}(\lambda' - \lambda)$ (Refs. 8 and 9), the solar constant $I_0(\lambda)$ (Ref. 10), and the ozone absorption coefficient.

Table I presents the values of the parameters β_j and n_j for three spectral channels, along with their errors $\Delta\beta_j$ and Δn_j. The zenith angles were taken varying from 30 to 75° in calculations of β_j and n_j. This Table was calculated using the model of midlatitude summer.

TABLE I.

λ_j, nm	β_j, nm	n_j	$\Delta\beta_j$	Δn_j
300	6.119502	0.713126	0.000179	0.000203
326	0.416949	0.982102	0.000080	0.000090
348	0.010966	0.995096	0.002320	0.002627

The problem of applicability of the data obtained (the values of the parameters β_j and n_j) to other atmospheric conditions has been studied. Toward this end, the direct problem was solved based on different ozone content models, while the inverse problem was solved based on the parameters presented in Table I. The simulation results have shown the maximum error in TOC reconstruction to be 0.06%.

With regard for Eq. (6), the model (5) takes the form

$$I(\lambda_j, \varphi) = C \exp\{(-\tau_{ma}(\lambda_j, \varphi) - \beta_j(W(\varphi))^{n_j}\}. \quad (8)$$

The numerical simulation has demonstrated that the deviation δI of the models (5) and (8) relative to Eq. (1) does not exceed 1.5% for the first filter, 0.4% for the second filter, and 0.1% for the third one.

In the wavelength range from 300 to 350 nm, the optical depth $\tau_{ma}(\lambda, \varphi)$ can be approximated by the following expression:

$$\tau_{ma}(\lambda, \varphi) = A(\varphi)\, (\lambda / \lambda_0)^{B(\varphi)}. \quad (9)$$

Having substituted Eq. (9) into Eq. (8), we obtain the final expression for the measured value:

$$I(\lambda_j, \varphi) = C \exp\{-A(\varphi)\, (\lambda_j / \lambda_0)^{B(\varphi)} - \beta_j(W(\varphi))^{n_j}\}. \quad (10)$$

Given the measured signals $I(\lambda_j, \varphi)$ at the three wavelengths, we can estimate three parameters A, B, and W from Eq. (10). Then we can find τ_{ma} from Eq. (9).

The angular dependence for the errors ΔA and ΔB is presented in Table II.

TABLE II.

φ	A	B	ΔA	ΔB
35.799999	1.556787	−3.179260	0.018848	0.191910
37.500000	1.591422	−3.179241	0.018847	0.191902
40.000000	1.647950	−3.179212	0.018847	0.191904

FAST ANALYSIS OF THE OZONE PROFILE

The technique described allows estimation of the ozone content and the optical depth $\tau_{ma}(\varphi)$ along the direction determined by the solar zenith angle φ. If $\varphi \le 50°$, then the function of a path in Eq. (7) can be replaced with sec φ, i.e.

$$W(\varphi) = \sec(\varphi)\ W_0, \qquad (11)$$

where W_0 is the total ozone content scaled to the vertical atmospheric column. At $\varphi > 50°$, the Earth's curvature should be taken into account. In the method of nomograms, $W(\varphi)$ is recalculated into W_0 by the corresponding nomograms. In this paper, we propose to determine not only W_0, but also some characteristics of the ozone profile, such as the effective height of the ozone layer H_0 and its depth d ($d = 2\sigma$, Fig. 2). Let us consider the method of obtaining H_0 and d.

Let there be $W(\varphi)$ for three values of the angles φ_i, $i = 1, 2, 3$. Then, having expanded the function of path in Eq. (7) into a power series over the parameter h/R, we obtain

$$\frac{(R + h)\ \rho(h)}{\sqrt{(R + h)^2 - R^2 \sin^2 \varphi}} = \rho(h) \times$$

$$\times\left\{1 + \left(\frac{h}{R}\right)\tan^2\varphi + \left(\frac{h}{R}\right)^2 \sec^2\varphi\left[\left(\frac{3}{2}\right)\sec^2\varphi - 1\right] + \ldots\right\}. \qquad (12)$$

Once integrated, Eq. (12) gives the following set of equations in the moments:

$$\mu_i = \int_0^{H_{atm}} h^i\ \rho(h)\ dh,$$

$$\begin{cases} \mu_0 - a_1\ \mu_1 + B_1\ \mu_2 = y_1, \\ \mu_0 - a_2\ \mu_1 + B_2\ \mu_2 = y_2, \\ \mu_0 - a_3\ \mu_1 + B_3\ \mu_2 = y_3, \end{cases} \qquad (13)$$

where

$$a_i = \frac{1}{R}\tan^2\varphi; \quad B_i = \frac{1}{R^2}\sec^2\varphi_i\left(\frac{3}{2}\sec^2\varphi_i - 1\right); \quad y_i = W(\varphi_i).$$

The solution of the set of equations (13) has the following form:

$$\mu_0 = \frac{1}{D} D_1; \quad \mu_1 = \frac{1}{D} D_2; \quad \mu_2 = \frac{1}{D} D_3, \qquad (14)$$

where

$$D = B_1(a_2 - a_3) + B_2(a_3 - a_1) + B_3(a_1 - a_2);$$

$$D_1 = y_1(a_3\ B_2 - a_2\ B_3) + y_2(a_1\ B_3 - a_3\ B_1) +$$

$$+ y_3(B_1\ a_2 - a_1\ B_2);$$

$$D_2 = y_1(B_2 - B_3) + y_2(B_3 - B_1) + y_3(B_1 - B_2);$$

$$D_3 = y_1(a_2 - a_3) + y_2(a_3 - a_1) + y_3(a_1 - a_2).$$

The ozone profile characteristics are related to the moments μ_i by the following relations:

$$W_0 = \mu_0 = \int_0^{H_{atm}} \rho(h)\ dh; \quad H_0 = \frac{\mu_1}{\mu_0} = \frac{\int_0^{H_{atm}} h\ \rho(h)\ dh}{\int_0^{H_{atm}} \rho(h)\ dh};$$

$$d = 2\sqrt{\frac{\mu_2}{\mu_0} - \left(\frac{\mu_1}{\mu_0}\right)^2}; \qquad (15)$$

where H and d are the effective height and depth of the ozone layer.

If the values of $W(\varphi)$ are measured only at two angles φ_i, $i = 1, 2$, then only two moments can be found from the experimental data:

$$\mu_0 = \frac{y_1\ a_2 - y_2\ a_1}{a_2 - a_1}; \quad \mu_1 = \frac{y_1 - y_2}{a_2 - a_1}, \qquad (16)$$

what is quite sufficient for estimating W_0 and H_0 from Eq. (15).

The estimation errors for the moments and the corresponding characteristics of the ozone profile are calculated by the following expressions.

a) Two-angle technique

$$\delta_{\mu_0} = \frac{\sqrt{\sigma_{Y_1}^2\ a_2^2 + \sigma_{Y_2}^2\ a_1^2}}{y_1\ a_2 - y_2\ a_1}; \quad \delta_{\mu_1} = \frac{\sqrt{\sigma_{Y_1}^2 + \sigma_{Y_2}^2}}{y_1 - y_2}; \qquad (17)$$

$$\delta_{W_0} = \delta_{\mu_0}; \quad \delta_{H_0} = \sqrt{\delta_{\mu_0}^2 + \delta_{\mu_1}^2 - 2\frac{1}{\mu_1\ \mu_0}\langle\Delta\mu_0\ \Delta\mu_1\rangle}, \qquad (18)$$

where

$$\langle\Delta\mu_0\ \Delta\mu_1\rangle = [(\sigma_{Y_1}^2\ a_2 + \sigma_{Y_2}^2\ a_1)]\ \frac{1}{(a_2 - a_1)^2}. \qquad (19)$$

Here $\sigma_{Y_i}^2$ is the measurement error of $y_i = W(\varphi_i)$.

B) Three-angle technique

$$\sigma_{\mu_0} = \frac{1}{D}\left\{\sigma_{Y_1}^2\ (a_3\ B_2 - a_2\ B_3)^2 + \sigma_{Y_2}^2\ (a_1\ B_3 - a_3\ B_1)^2 + \right.$$

$$\left. + \sigma_{Y_3}^2\ (a_2\ B_1 - a_1\ B_2)\right\}^{1/2};$$

$$\sigma_{\mu_1} = \frac{1}{D}\left\{\sigma_{Y_1}^2\ (B_2 - B_3)^2 + \sigma_{Y_2}^2\ (B_3 - B_1)^2 + \right.$$

$$\left. + \sigma_{Y_3}^2\ (B_1 - B_2)\right\}^{1/2};$$

$$\sigma_{\mu_2} = \frac{1}{D}\left\{\sigma_{Y_1}^2\ (a_2 - a_3)^2 + \sigma_{Y_2}^2\ (a_3 - a_1)^2 + \right.$$

$$\left. + \sigma_{Y_3}^2\ (a_1 - a_2)\right\}^{1/2}.$$

The errors δ_{W_0} and δ_{H_0} are calculated by Eq. (18), in which

$$\delta_{\mu_i} = \frac{\sigma_{\mu_i}}{\mu_i}, \quad i = 1, 2;$$

$$\langle\mu_0\ \mu_1\rangle = \frac{1}{D^2}\left\{\sigma_{Y_1}^2\ (a_3\ B_2 - a_2\ B_3)\ (B_2 - B_3) + \right.$$

$$+ \sigma_{Y_2}^2\ (a_1\ B_3 - a_3\ B_1)\ (B_3 - B_1) +$$

$$\left. + \sigma_{Y_3}^2\ (a_2\ B_1 - a_1\ B_2)\ (B_1 - B_2)\right\}. \qquad (20)$$

Let us estimate the error

$$\sigma_d = 2\frac{1}{d}\left\{ \delta^2_{\mu 0}\left[\frac{\mu_2}{\mu_0} - 2\left(\frac{\mu_1}{\mu_0}\right)^2 \right]^2 + \delta^2_{\mu 1}\, 4\left(\frac{\mu_1}{\mu_0}\right)^4 + \right.$$

$$+ \delta^2_{\mu 2}\left(\frac{\mu_2}{\mu_0}\right)^2 + 4\left(\frac{\mu_2}{\mu_0}\right)\left(\frac{\mu_1}{\mu_0}\right)^2 \times$$

$$\times\left[\frac{1}{\mu_0\,\mu_1} <\Delta\mu_0\,\Delta\mu_1> - \frac{1}{\mu_1\,\mu_2} <\Delta\mu_1\,\Delta\mu_2> \right] +$$

$$\left. + 2\frac{1}{\mu_0^2}\left[2\left(\frac{\mu_1}{\mu_0}\right)^2 - \frac{\mu_2}{\mu_0} \right] <\Delta\mu_0\,\Delta\mu_2> \right\}^{1/2}. \qquad (21)$$

Here $<\Delta\mu_0\,\Delta\mu_1>$ are calculated by Eq. (20)

$$<\Delta\mu_1\,\Delta\mu_2> = \frac{1}{D^2}\left\{\sigma^2_{Y_1}(B_2 - B_3)\,(a_2 - a_3) + \right.$$

$$\left. + \sigma^2_{Y_2}(B_3 - B_1)\,(a_3 - a_1) + \sigma^2_{Y_3}(B_1 - B_2)\,(a_1 - a_2)\right\}; \qquad (22)$$

$$<\Delta\mu_0\,\Delta\mu_2> = \frac{1}{D^2}\left\{\sigma^2_{Y_1}\,(a_3\,B_2 - a_2\,B_3)\,(a_2 - a_3) + \right.$$

$$+ \sigma^2_{Y_2}\,(a_1\,B_3 - a_3\,B_1)\,(a_3 - a_1) +$$

$$\left. + \sigma^2_{Y_3}\,(a_2\,B_1 - a_1\,B_2)\,(a_1 - a_2)\right\}. \qquad (23)$$

SIMULATED RESULTS

To study the potentialities of the proposed technique (the method of moments) in reconstruction of TOC, the height of the center of gravity of the ozone layer, and the halfwidth of the ozone layer, some numerical simulations have been performed. The function $W(\varphi)$ was simulated by integrated Gaussian curve with the parameters A, σ, and X_0 (simulation of the ozone layer by Gaussian curve and the meaning of the presented parameters are demonstrated in Fig. 2). Of interest was the dependence of the function $W(\varphi)$ on the parameters of Gaussian curve. A change in the parameter A characterizes the variation of the total content, while a change in σ is indicative of variations in the ozone layer halfwidth, and X_0 reflects the influence of the center of gravity (the effective height):

$$\omega(\varphi) = \frac{1}{\cos\varphi}\int f(x)\,dx;$$

$$f(x) = A\exp\left\{ -\frac{(x - x_0)^2}{2\,\sigma^2} \right\}.$$

Thus obtained results of simulations are shown in Figs. 3–5.

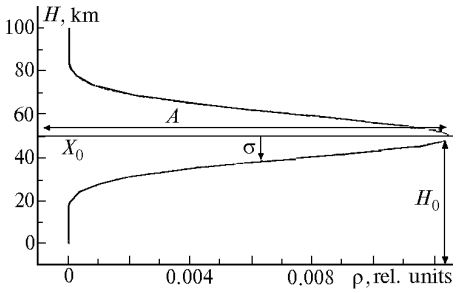

FIG. 2. The graphical Heaning of the paraHeters A, σ, and X_0, siHulating the paraHeters of the ozone layer.

As seen from the figures, an increase in the amplitude A (variation of the total content, Fig. 3), as well as the halfwidth σ (the layer halfwidth, Fig. 4), results in the corresponding increase of the function $W(\varphi)$. A variation of the parameter X_0 of Gaussian curve (the layer center of gravity, Fig. 5) has a weak influence on the function $W(\varphi)$.

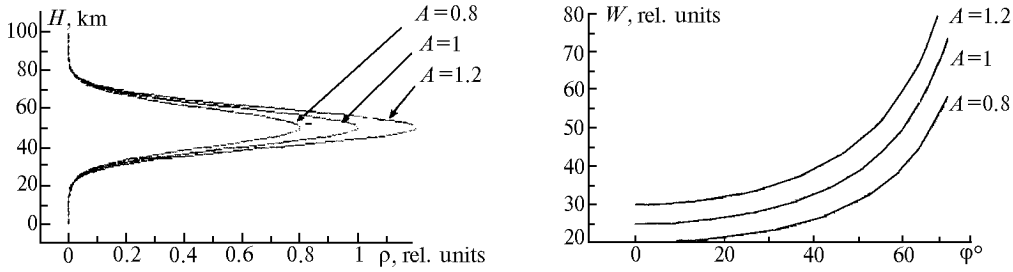

FIG. 3. Dependence of the function $W(\varphi)$ on the paraHeter A (siHulation of variation in the total ozone content).

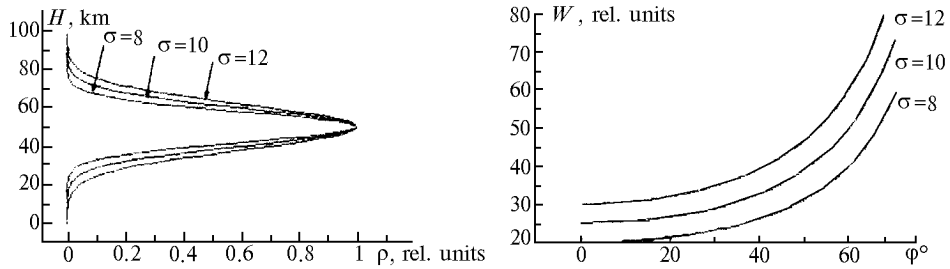

FIG. 4. Dependence of the function $W(\varphi)$ on the paraHeter σ (siHulation of variation in the halfwidth of the ozone layer).

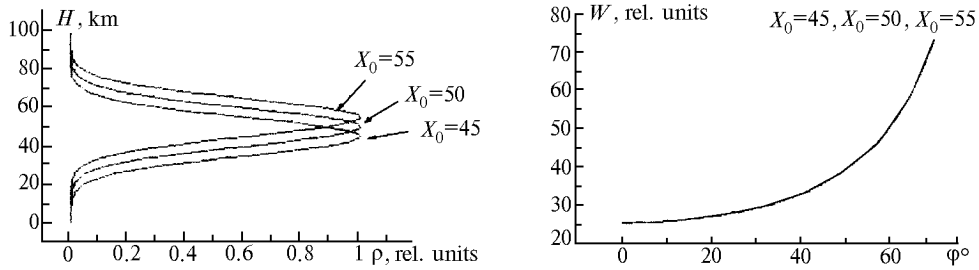

FIG. 5. Dependence of the function W(φ) on the paraHeter X_0 (siHulation of variation in the height of the ozone layer HaxiHuH).

PROCESSING OF THE FIELD DATA

To test the technique developed, we have processed data of real broad-band measurements conducted on May 24, 1998, with a M–124 device. The processed data on TOC reconstruction (the third column) are presented in Table III in comparison with the data on TOC obtained by the method of nomograms (the second column). "ecause the method of nomograms does not allow estimation of the ozone profile parameters, the parameters of the ozone layer presented in the Table III (the height of the layer center shown in the fourth column and the layer depth shown in the fifth column) were compared with the values of the sought parameters calculated on the basis of the midlatitude summer model.

TABLE III.

Solar zenith angle φ°	Measured TOC data	W_0	H_0	d
37.4				
37.9	0.345	0.34206	22.31653	29.14012
38.1				

According to model calculations

W_0 = 0.354 atm·cm; H_0 = 23.32 km; d = 9.27 km.

As seen from Table III, the results obtained are in a close agreement with the model calculations. The marked discrepancy for the reconstructed second moment (d) can be explained by small values of the solar zenith angle, because the technique is most accurate at large zenith angles (φ > 50°), i.e., when the function of a path $B(h, \varphi)$ differs sufficiently strong from $1/\cos(\varphi)$.

ACKNOWLEDGMENTS

In conclusion, the authors would like to express their gratitude to S.V. Smirnov for the measurement data acquired with a M–124 which he kindly presented at our disposal and to Professor S.D. Tvorogov for useful critical remarks.

REFERENCES

1. G.P. Gushchin, ed., *AtHospheric Ozone. Proc. of the Fourth All-Union SyHposiuH* (Gidrometeoizdat, Leningrad, 1987), 302 pp.
2. A.Kh. Khrgian, *Physics of AtHospheric Ozone* (Gidrometeoizdat, Leningrad, 1973), 291 pp.
3. L.T. Molina and M.J. Molina, J. Geophys. Res. **19**, No. D13, 14501–14508 (1986).
4. V.E. Zuev and V.S. Komarov, *Statistical Models of TeHperature and Gaseous CoHponents of the AtHosphere* (D. Reidel, Dodredrect–"oston–Lancaster–Tokyo, 1987), 306 pp.
5. I.L. Karol', V.V. Rozanov, and Yu.M. Timofeev, *Gaseous AdHixtures in the AtHosphere* (Gidrometeoizdat, Leningrad, 1983), 223 pp.
6. G.M. Krekov and R.F. Rakhimov, *Optical Models of AtHospheric Aerosol* (Tomsk, 1986), 294 pp.
7. I.I. Ippolitov, V.S. Komarov, and A.A. Mitsel', in: *Spectroscopic Methods for Sounding of the AtHosphere* (Nauka, Novosibirsk, 1985), pp. 4–44.
8. G.P. Gushchin and N.N. Vinogradova, *Total Ozone in the AtHosphere* (Gidrometeoizdat, Leningrad, 1977), 238 pp.
9. I.M. Nazarov, A.I. Nikolaev, and Sh.D. Fridman, *ReHote and Fast Methods for Detection of EnvironHental Pollution* (Gidrometeoizdat, Leningrad, 1977), 195 pp.
10. M.P. Thekaekara, Appl. Opt. **13**, No. 3, 518–522 (1974).